Arabian Journal for Science and Engineering (2020) 45:7835–7849
https://doi.org/10.1007/s13369-020-04725-x

RESEARCH ARTICLE-PETROLEUM ENGINEERING

Collaborative Design of the Wrap Angles Between Impeller and Space Diffuser of Diagonal-Flow Pump

Yingju Pei[1] · Qingyou Liu[2,3] · Guorong Wang[2] · Wenwu Song[4]

Received: 19 May 2019 / Accepted: 26 December 2019 / Published online: 21 July 2020

Abstract

The wrap angle is one of the key parameters in design of impeller and space diffuser. At present, it is mainly designed based on theoretical estimation and experience. However, there are few studies on collaborative design. In this paper, the process model of collaborative design was put forward, then 25 kinds of wrap angle matching schemes between impeller and space diffuser were determined by orthogonal experimental method, and it was completed to study basic change law of the external characteristics and flow field under different matching schemes. It was shown that impeller wrap angle had more obvious influence on the hydraulic characteristics than space diffuser wrap angle within a certain wrap angle range. Therefore, the optimal impeller wrap angle should be determined in the collaborative design at first. By the multidimensional evaluation criteria, it was carried out such as the selection of the space diffuser wrap angle. It can reduce a lot of work to easily find a better balance about multi-influence of the multi-component parameters, and get an optimal performance when the diagonal-flow pump is used in oil and gas development.

Keywords Diagonal-flow pump · Oil and gas · Collaborative design · Impeller · Space diffuser · Wrap angle

1 Introduction

The diagonal-flow pump is widely used in petrochemical industry, onshore petroleum engineering, offshore oil and gas development, and other fields. It is a kind of pump whose characteristic and structure are between the axial-flow pump and the centrifugal pump, known as the guide vane mixed-flow pump. It has many advantages such as small outer diameter, convenient maintenance and disassembly, strong cavitation resistance, and high efficiency.

✉ Qingyou Liu
liuqy66@aliyun.com

✉ Guorong Wang
swpi2002@163.com

1 Petroleum Engineering School, Southwest Petroleum University, Chengdu 610000, China

2 State Key Laboratory of Oil and Gas Reservoir Geology and Exploitation, Southwest Petroleum University, Chengdu 610000, China

3 Chengdu University of Technology, Chengdu 610000, China

4 School of Energy and Power Engineering, Xihua University, Chengdu 610000, China

Impeller and space diffuser are main parts of diagonal-flow pump, and the optimum design plays a vital role in increasing the hydraulic characteristics when the diagonal-flow pump is used in oilfield engineering [1–3]. It should be studied in the collaborative design of key parameters by multidimensional analysis, not just confined to analyze single factor [4, 5]. Heo et al. [6] showed that the efficiency of the mixed-flow pump at the prescribed specific speed was improved considerably by the design optimization. Tan et al. [7] analyzed the influence of blade wrap angle on centrifugal pump performance by numerical and experimental study. Liu et al. [8] studied the influence of geometry of inlet guide vanes on pressure fluctuations of a centrifugal pump. According to the studies, the optimal hydraulic performance of the whole system can be obtained only by designing the best matching scheme of impeller and space diffuser. Therefore, the collaborative design of the wrap angles between impeller and space diffuser is very important.

At present, there are many research results on the single parameter of impeller and space diffuser. Kim et al. [9] found the effects of two geometric variables related to the area of the discharge and length of the vane in the diffuser on the efficiency of a mixed-flow pump. Bing et al. [10] carried out experimental study of the influence of flow passage

subtle variation on mixed-flow pump performance. Ofuchi et al. [11] studied the effect of viscosity on the head and flow rate degradation in different multistage electric submersible pumps using dimensional analysis. Lu et al. [12] proposed a new design approach to the radial pump's meridional channel design. Samad et al. [13] demonstrated that using multiple surrogates could improve the robustness of the optimization at a minimal computational cost. Wang et al. [14] studied the intelligence design method for three-dimensional vane diffusers in a centrifugal compressor. Bonaiuti et al. [15] showed the capability of this design strategy to perform the three-dimensional. Chen et al. [16] analyzed the influences of blade parameters and three-dimensional configuration on pressure distribution of the blades' suction surfaces.

However, there are few studies on the collaborative design between them. Based on an RBNN model, Kim et al. [17] put forward an optimization procedure for a vane diffuser design in a mixed-flow pump. Kim et al. [18] studied the multi-objective optimization of a centrifugal compressor impeller through evolutionary algorithms. The mutual relationship between the impeller and space diffuser remains on the basis of their respective optimization. The wrap angle is one of the key parameters, and it is particularly important in the collaborative design of impeller and space diffuser.

Therefore, in this paper, it was taken to study wrap angles of impeller and space diffuser and analyze vortex and cavitation in the diagonal-flow pump with different matching schemes. The best matching method of wrap angles in the impeller and space diffuser was researched, and the concepts of collaborative design about diagonal-flow pump were put forward.

2 Collaborative Design and Matching Schemes

2.1 Collaborative Design

The collaborative design of pump refers to the comprehensive consideration of the interaction among various factors and obtains optimal hydraulic characteristics by researching the optimal matching scheme of influencing factors. The research results of single parameter show that it should be focused on both the in-depth exploration of the matching effect among the main parameters and more comprehensively optimization of the structure design to finally obtain the optimal hydraulic performance of pump.

Figure 1 shows the collaborative design flow of the wrap angle between impeller and space diffuser. Based on design experience [19], the impeller wrap angle φ_i is taken from φ_1 to φ_n, and the space diffuser wrap angle φ_s is taken from φ_1' to φ_n', which are made into $\varphi = \varphi(\varphi_i, \varphi_s, k_\varphi)$ by linear combination. Then, the simulation is carried out to comprehensively

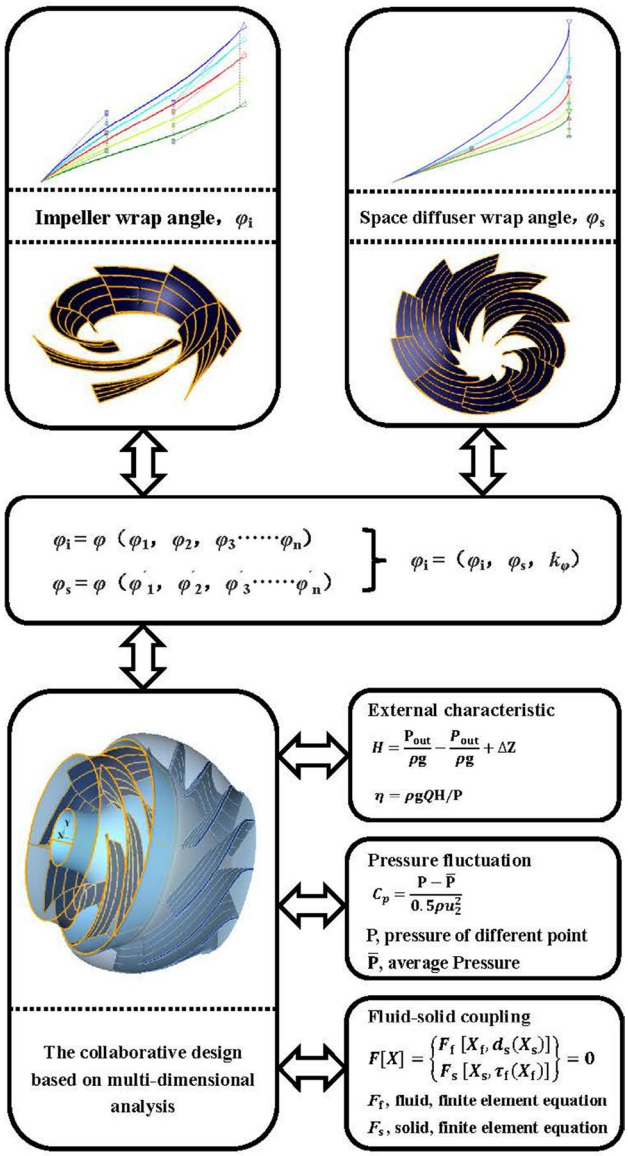

Fig. 1 Diagram of wrap angle co-design of diagonal-flow pump

analyze the change law of the hydraulic performance under different matching schemes of wrap angle between impeller and space diffuser. Finally, the hydraulic performance of every matching scheme is statistically analyzed by using the relationship formula $\varphi_{\eta,h} = \varphi(\varphi_i, \varphi_s, k_{\eta,h})$, so as to deeply explore the law of wrap angle matching between impeller and space diffuser.

Figure 2 shows the process of collaborative design between impeller and space diffuser: (1) In the range of empirical design, tasks are carried out successively, such as selecting the wrap angles of impeller and space diffuser, establishing 3D model with different wrap angles, analyzing the hydraulic characteristics and the whole flow field by numerical simulation, summing up the influence law of

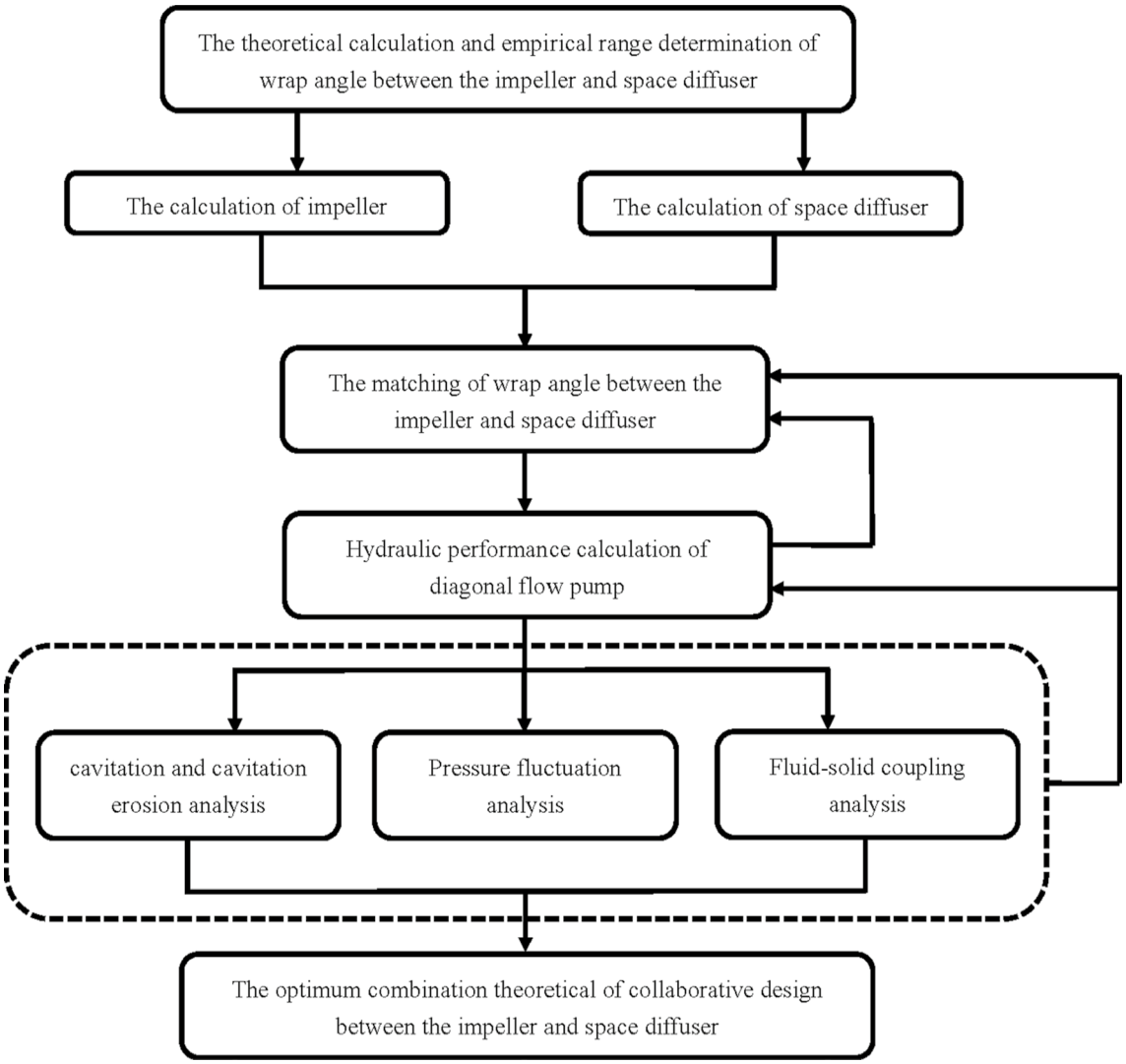

Fig. 2 Flowchart of wrap angle co-design of diagonal-flow pump

different wrap angles on hydraulic characteristics by statistically comparing the hydraulic performance of every matching scheme with $\varphi_{\eta,\mathrm{h}} = \varphi(\varphi_\mathrm{i}, \varphi_\mathrm{s}, k_{\eta,\mathrm{h}})$, and selecting a better range of values. (2) In the second part, tasks such as matching the wrap angle between the impeller and space diffuser by adopting orthogonal method, analyzing the hydraulic characteristics of the whole flow field in the every matching scheme by correcting formula $\varphi = \varphi(\varphi_\mathrm{i}, \varphi_\mathrm{s}, k_\varphi)$, and selecting the better matching scheme based on the statistical comparison of every hydraulic performance are carried out successively. (3) Finally, the tasks are carried out successively, such as summarizing the selection criteria of key influencing factors and secondary influencing factors by multidimensional evaluating the selected matching scheme, and putting forward the mechanism of wrap angles co-design to provide reference for improving operation performance of diagonal-flow pump.

The above collaborative design process provides a detailed guidance in the development and optimization of a new pump model. At the same time, according to the special requirements of the characteristics of diagonal-flow pump under different application conditions, there are three parts of hydraulic characteristics in the collaborative process. Some parts of them need to be carried out with emphasis, so that the research and development cycle is reduced, and collaborative design has strong pertinence to achieve high goals.

2.2 Matching Schemes of Wrap Angle

The wrap angle is one of the key parameters in design of impeller and space diffuser, which is mainly a range determined by theoretical estimation and experience. The recommended impeller wrap angle of the diagonal-flow pump

ranges from 70° to 110°, and the recommended space diffuser wrap angle of the diagonal-flow pump ranges from 40° to 80°. Based on the influence law and inducing mechanism among different wrap angles of impeller and space diffuser, respectively, the matching schemes of different wrap angles are carried out. Within the range of the recommended wrap angle, the impeller wrap angle φ_i takes 70°, 80°, 90°, 100°, and 110°. The space diffuser wrap angle φ_s takes 40°, 50°, 60°, 70°, and 80°. Then, linear combinations between φ_i and φ_s are carried out, and there are 25 schemes as shown in Tables 1 and 2.

Based on the linear combination of 25 matching schemes, the tasks are carried out, such as finishing the simulation analysis of every scheme, analyzing the change law of

Table 1 Horizontal combination of φ_i and φ_s

No.	Scheme	φ_i/φ_s	No.	Scheme	φ_i/φ_s
1	A1	70°/40°	6	B1	80°/40°
2	A2	70°/50°	7	B2	80°/50°
3	A3	70°/60°	8	B3	80°/60°
4	A4	70°/70°	9	B4	80°/70°
5	A5	70°/80°	10	B5	80°/80°
No.	Scheme	φ_i/φ_s	No.	Scheme	φ_i/φ_s
11	C1	90°/40°	16	D1	100°/40°
12	C2	90°/50°	17	D2	100°/50°
13	C3	90°/60°	18	D3	100°/60°
14	C4	90°/70°	19	D4	100°/70°
15	C5	90°/80°	20	D5	100°/80°
No.		Scheme			φ_i/φ_s
21		E1			110°/40°
22		E2			110°/50°
23		E3			110°/60°
24		E4			110°/70°
25		E5			110°/80°

Table 2 Longitudinal combination of φ_i and φ_s

No.	Scheme	φ_i/φ_s	No.	Scheme	φ_i/φ_s
1	H1	70°/40°	6	I1	70°/50°
2	H2	80°/40°	7	I2	80°/50°
3	H3	90°/40°	8	I3	90°/50°
4	H4	100°/40°	9	I4	100°/50°
5	H5	110°/40°	10	I5	110°/50°
No.	Scheme	φ_i/φ_s	No.	Scheme	φ_i/φ_s
11	J1	70°/60°	16	K1	70°/70°
12	J2	80°/60°	17	K 2	80°/70°
13	J3	90°/60°	18	K3	90°/70°
14	J4	100°/60°	19	K4	100°/70°
15	J5	110°/60°	20	K5	110°/70°
No.		Scheme			φ_i/φ_s
21		L1			70°/80°
22		L2			80°/80°
23		L3			90°/80°
24		L4			100°/80°
25		L5			110°/80°

hydraulic performance under different matching schemes about the wrap angles, and exploring the matching law of the wrap angles between the impeller and space diffuser.

3 Model Parameters and Experimental Validation

3.1 Model Parameters

The basic parameters of the diagonal-flow pump studied in this paper are rated flow $Q = 120$ m^3/h, head $H = 10$ m, and speed $n = 2900$ r/min. The 3D model of solid domain and fluid domain is shown in Fig. 3.

3.2 Boundary Conditions and Experimental Validation

In recent years, some scholars have focused on the effects of different turbulence models on the performance prediction and flow calculation of mixed-flow pump [20–22]. Diagonal-flow pump is also called guide vane mixed-flow pump, so the research results offer important referential value and illumination. Among them, Bing et al. [23] simulated the turbulent flow in the whole channel by standard k-ε, RNG k-ε, k-ε, and SST k-ε turbulence models, respectively, and compared with the experimental results to evaluate the effect of predicting the external characteristics of each turbulent model. The results showed that RNG k-ε model was more accurate under (0.9–1.3) Q_d conditions.

Different calculation models have certain application conditions. Under different objects and conditions, the applicability of the calculation model is also different. Five different approaches to turbulent flow for choosing large eddy simulation (LES) method have been investigated and analyzed from studies, and the pre-calculation of each calculation model has been carried out, such as standard k-ε, RNG k-ε, k-ε, and SST k-ε turbulence models. The RNG k-ε model considers the rotation and swirl in the mean flow by modifying the turbulent viscosity, and a term reflecting the time-averaged strain rate of the mainstream is added to the equation. Thus, the RNG k-ε model can better deal with the flow with swirl, high strain rate, and high curvature of streamline. RNG k-ε model can adapt to different wrap angle ranges well. It has high agreement with the experiment under different flow rates. Then, the research results and model pre-calculation show that the RNG k-ε model is closer to the experimental under (0.8–1.4) Q_d conditions, especially for diagonal-flow pump. Therefore, considering the calculation accuracy of hydraulic characteristics and large curvature blade passage vortices, and the calculation time efficiency, RNG k-ε model is chosen to analyze the turbulence inside the diagonal-flow pump.

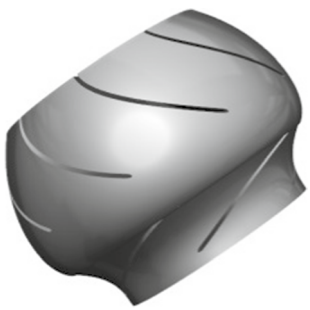

Fig. 3 3D model of impeller and space diffuser

The governing equations for fluid motion use a three-dimensional, steady, incompressible Reynolds-averaged Navier–Stokes equations, and the RNG k-ε turbulence model.

Constraint equation of turbulent kinetic energy

$$\frac{\partial(\rho k)}{\partial t} + \frac{\partial(\rho k u_j)}{\partial x_j} = \frac{\partial}{\partial x_j}\left(\alpha_k \mu_e \frac{\partial k}{\partial x_j}\right) + \rho(P_k - \varepsilon). \tag{1}$$

Constraint equation of turbulent dissipation rate

$$\frac{\partial(\rho \varepsilon)}{\partial t} + \frac{\partial(\rho \varepsilon u_j)}{\partial x_j} = \frac{\partial}{\partial x_j}\left(\alpha_\varepsilon \mu_e \frac{\partial \varepsilon}{\partial x_j}\right) + \rho \frac{\varepsilon}{k}(C^*_{1\varepsilon} P_k - C_{2\varepsilon}\varepsilon). \tag{2}$$

Based on the research results of previous similar simulation, the three-dimensional model of the flow field established above was imported into ICEM for meshing. An unstructured tetrahedral grid was used, and the grid encryption at blade tip and other areas with small transition angles was carried out to ensure the mesh's overall quality (above 0.4) and the accuracy of numerical calculations, as shown in Fig. 4. Then, the model is pre-calculated and analyzed by CFX to ensure that the grid generation quality matches the experimental results. The iteration residual is set to 10^{-4}. At the same time, based on the difference between the average mass flow of the inlet and outlet being less than 0.5% and the weighted average total pressure at the monitoring outlet, the above three monitoring conditions are comprehensively analyzed to determine the convergence of the calculation results. According to statistics, the total number of grids is 5.6 million. Considering the calculation time and the reliability of the calculation results, when the number of grids is increased again, the error of the calculation results is within 1.9%, which meets the requirements of simulation calculation.

The boundary conditions: no slip wall, pressure inlet, mass outflow, and so on. In addition, the standard RNG k-ε model is selected, and the SIMPLEC algorithm is used to simulate the internal flow of the diagonal-flow pump. At the same time, reference experiment validation

Fig. 4 Meshing

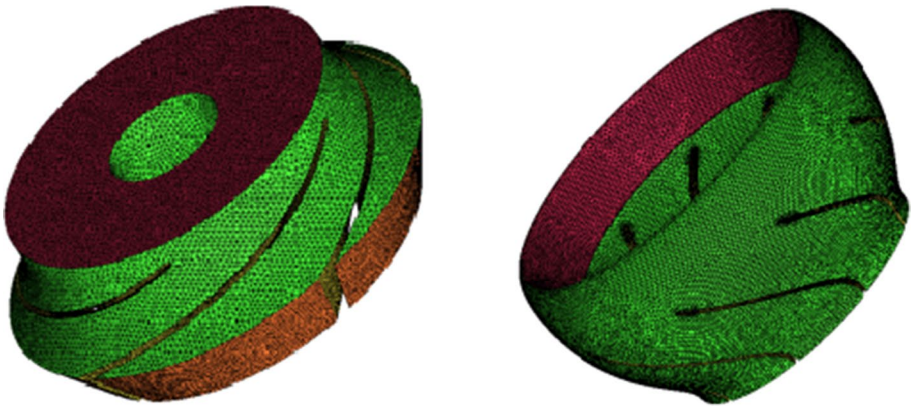

(a) Impeller fluid domain grid **(b)** Space diffuser fluid domain grid

Table 3 Experimental instrument

Serial number	Name	Instrument number
1	Vacuum pressure gauge(−0.1 to 0.3 Mpa)	11.05.28.9201
2	Precision pressure gauge(0–1 Mpa)	09.8.113
3	Pressure transmitter-1(−0.1 to 1 Mpa)	CZZA052681635
4	Pressure transmitter-2(−0.1 to 1 Mpa)	S4HCC01236851
5	Vortex flowmeter	14111624

is carried out. The experimental pump is diagonal-flow pump with space diffuser. The inlet diameter is 347 mm, the outlet diameter is 252 mm, the impeller diameter is 441.5 mm, the number of blades is seven, and the head is 50 m. An intelligent vortex flowmeter is used for flow measurement, and other experimental instruments are shown in Table 3. In order to ensure the reliability of the experimental results, multiple experiments and multiple measurements are performed to eliminate errors caused by accidental factors.

Through data processing and data fitting, the comparison between experiment and calculation is shown in Fig. 5. The calculation method is validated by experiment. The head and efficiency curve were analyzed under the different flow conditions near designed working condition [24]. The average error of efficiency is within 1.4% and the average error of head is within 1.1%, which meet the analysis requirements. It was also proved that the calculation settings and simulation results are reliable, which can be used for reference for calculation and analysis.

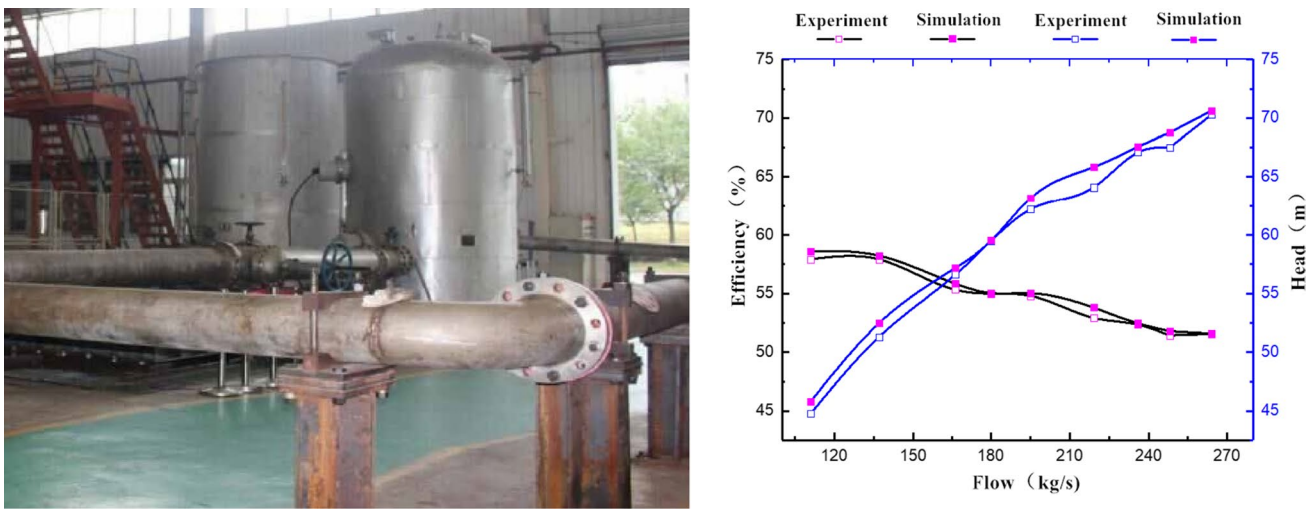

(a) Test-bed **(b)** Result analysis

Fig. 5 Comparison of experiment and simulation

4 Result Analysis

4.1 External Characteristics Analysis

Through numerical calculation, the efficiency curves of 25 schemes are obtained, and the horizontal and vertical curves are carried out, as shown in Fig. 6.

It can be seen from the efficiency curves of horizontal and vertical groups: (1) A, B, C, D, and E five horizontal schemes are based on impeller wrap angles, B and C are the higher efficient, and the higher efficiency area is wider. For example, the efficiencies of C2, C3, and C4 in group C are 85.04%, 85.44%, and 85.18%, respectively, all in the range of higher efficiency, while the highest efficiency points of group A with smaller wrap angle are shifted to the left, and the highest efficiency points of group E with larger wrap angle are shifted to the right. (2) H, I, J, K, and L vertical schemes are based on space diffuser wrap angles, the five groups all show "saddle shape," and the highest efficiency points are more consistent in the same y-coordinate position, but the higher efficiency area is narrow, and the downward trend of the highest point is steep. For example, the efficiencies of J2, J3, and J4 in group J are 83.53%, 85.44%, and 80.74%, respectively, and the long-span is from 80 to 86%, indicating that the impeller wrap angle has more obvious effect on the overall efficiency than the space diffuser wrap angle. In the certain wrap angle range near the highest point efficiency, the impact of space diffuser wrap angle is relatively small, exhibiting a high-efficiency region.

In order to more conveniently and intuitively analyze the head and efficiency of every combination scheme in the horizontal and vertical groups, the head curves were drawn, as shown in Fig. 7.

It can be seen from Fig. 7: (1) The heads of A, B, C schemes all meet the design head requirements, and they are basically coincide with the trend of the efficiency curves in Fig. 6. When the wrap angle is small, it is shifted to the left. When the wrap angle is large, it is shifted to the right. But groups D and E are all below 8.5 m, which is lower than the design head. (2) The change trends of the five groups are all the same, first increase and then decrease greatly. For example, J1 = 10.41 m, J2 = 11.01 m, J3 = 10.60 m, J4 = 8.40 m, and J5 = 8.40 m in group *J*. The highest heads are consistent in lateral coordinate, respectively, H2 = 10.57 m, I2 = 10.93 m, J2 = 11.01 m, K2 = 11.05 m, and L2 = 10.92 m. After the highest point, head curves are steeply steep in the schemes that the impeller wrap angles are relatively large. These show that the optimal efficiency in a certain wrap angle range should not be the only concern, but also whether the head meets the design requirements is considered, so as to ensure the optimal operation of the diagonal-flow pump in the complex multi-environment under the actual working conditions.

4.2 Internal Flow Field and Fluid–Solid Coupling

Based on the horizontal and vertical external characteristics analysis of the above-mentioned 25 cooperative design schemes, it has already illustrated the necessity and significance of collaborative design. Because ten combinations of A and E groups deviate from the initial performance requirements of the diagonal-flow pump, these were given up. In order to efficiently and comprehensively analyze the wrap angle schemes, nine groups of wrap angle combinations in the representative groups B, C, and D were selected

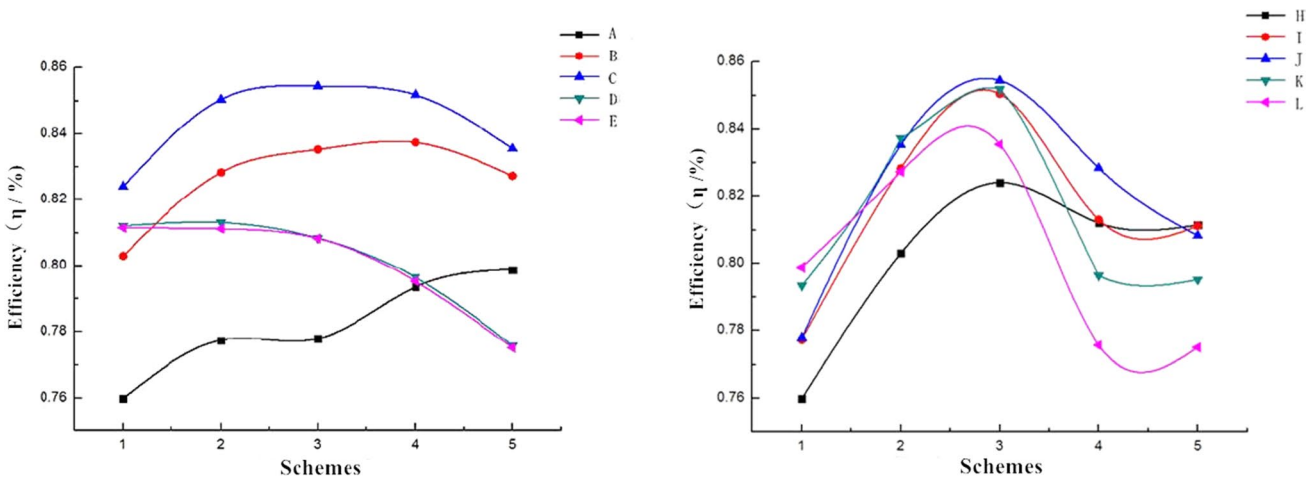

(a) Efficiency curve in horizontal

(b) Efficiency curve in vertical

Fig. 6 Efficiency curve of every group

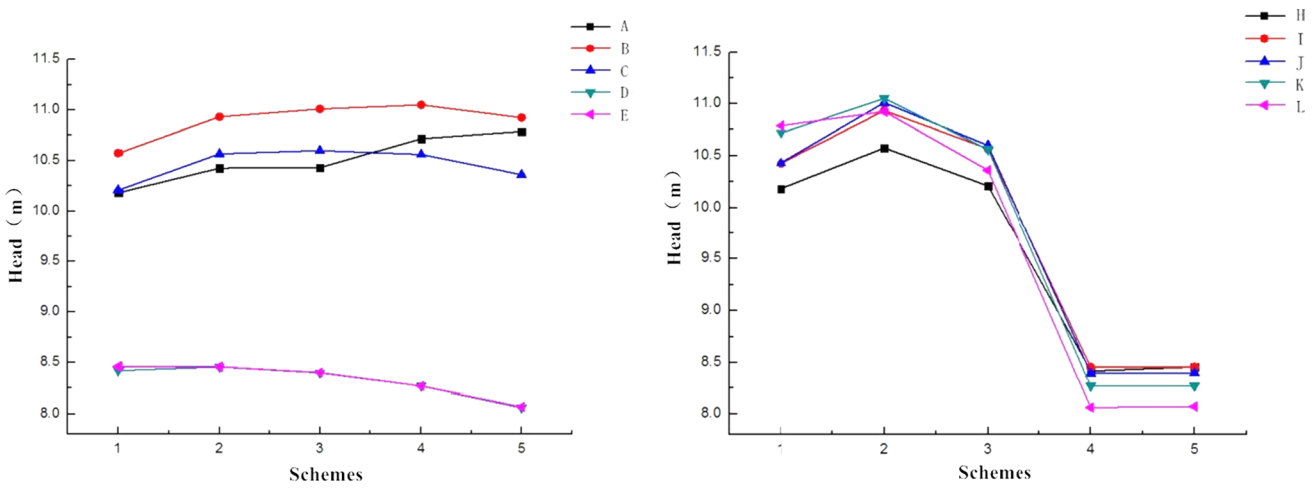

(a) The head curves in lateral

(b) The head curves in lengthwise

Fig. 7 Head curves

to analyze the internal flow field of the space diffuser and further explore the influence law and internal mechanism of overall performance under the different cooperative design wrap angle schemes. As shown in Fig. 8, the cross section at 0.08 m of the impeller inlet is established.

The streamline and pressure contours of the Sect. 1 in the diagonal-flow pump are compared in Fig. 9. It can be seen that: (1) The low-pressure area of the three schemes in group D is larger than that in groups B and C. The pressure distribution of the six schemes is consistent with the section of the space diffuser flow channel, indicating that the influence of wrap angle schemes between the impeller and space diffuser is mutually and tightly unified. In the design and analysis, the overall consideration is needed, and the system should be integrated. (2) The change in the space diffuser wrap angle has a great influence on the internal flow field of the space diffuser. Within the range of the small wrap angles, the reflux and vortex are obvious. With the increase in the wrap angle, the internal flow field of the space diffuser is relatively smooth and the reflux and vortex are significantly reduced. However, the external characteristics are the result of the interaction among the main components of the impeller and space diffuser. Therefore, the internal flow field should be comprehensively considered in analysis of the internal factors. In the meantime, it needs to be balanced that the flow separation on the blade surface will gradually reduce as the wrap angle increases. But when the wrap angle is too large, the friction loss between the fluid and the blade surface will obviously increase. Therefore, on the basis of the balance about multi-influence of the single key parameters, the collaborative design can also find a better balance point about multi-influence of the parameters.

Based on the numerical results of the above flow field, the fluid–solid coupling module is constructed in Workbench. The fluid–solid coupling of impeller and space diffuser is set up under different flow conditions, and the speed of impeller is 2900r/min. The fluid–solid coupling surface is selected as blade surface and inner surface of front and rear covers, and constraints are added to carry out numerical calculation of fluid–solid coupling.

As can be seen from Figs. 10 and 11, under different flow conditions: (1) The maximum deformation of the impeller front cover is much larger than that of the rear cover, and the deformation of impeller gradient increases along the hub radial direction. The maximum deformation is located at the exit edge of the front cover of the impeller outlet, which is at the dynamic-static junction. After obtaining high-speed kinetic energy, the fluid is discharged through space diffuser passage. (2) The maximum stress and deformation of space diffuser decrease

Fig. 8 Section view

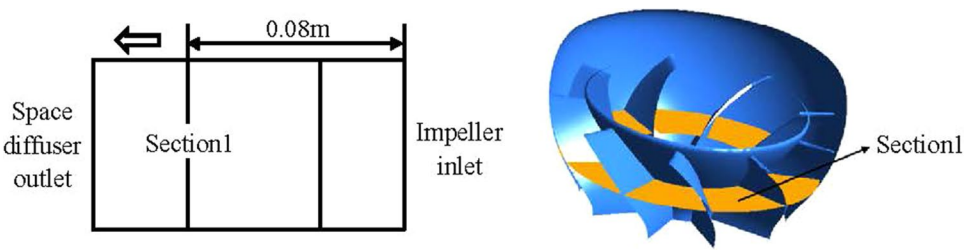

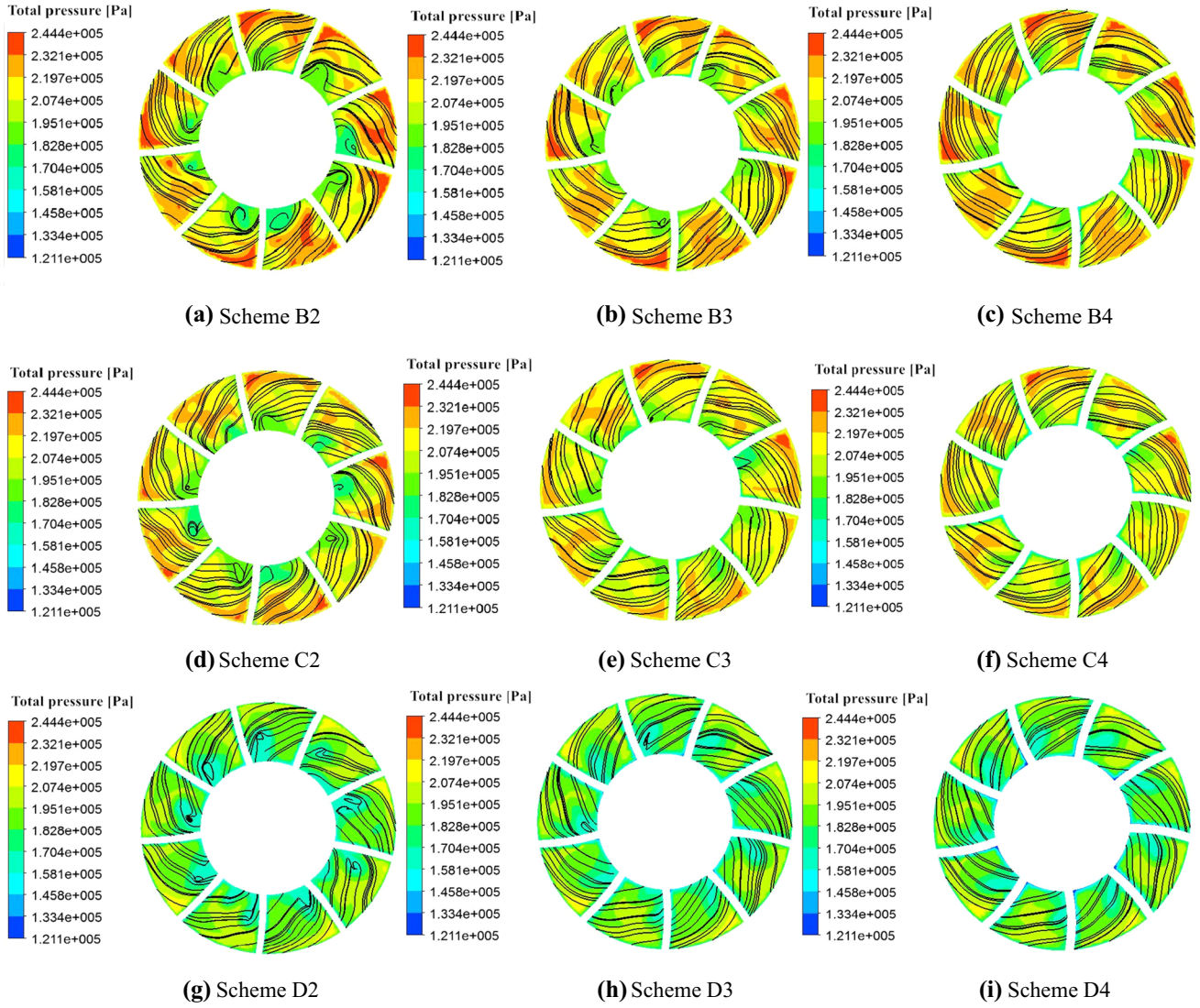

Fig. 9 Streamline and pressure contours of different wrap angles in Sect. 1

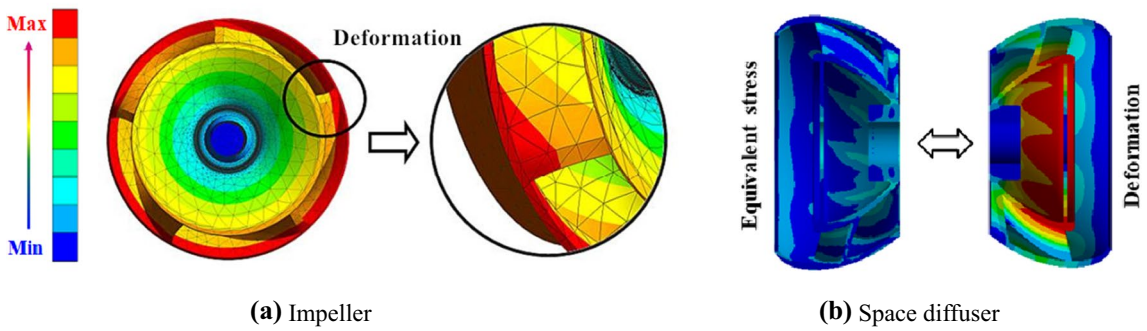

Fig. 10 Coupling deformation and stress

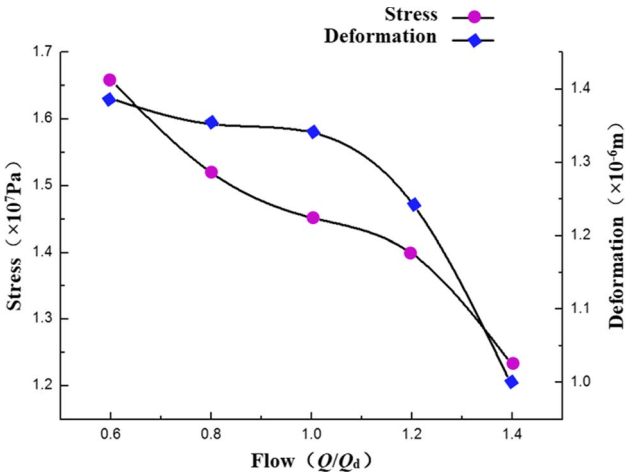

Fig. 11 Maximum stress and deformation of space diffuser under different flows

with the increase in flow. The stress is mainly concentrated on the inlet edge of the front cover and the connection between the guide blade and cover, which is strongly impacted by the fluid. However, due to the restraint of rigid connections, the stress cannot be effectively released, resulting in a larger stress.

In the design process, besides ensuring the transition between the guide blade and the cover as far as possible, the strength design of the middle position of the two guide blades on the front cover should be considered.

4.3 Cavitation Analysis

Design condition is one of the key conditions to ensure optimal hydraulic characteristic in design process of pump. Large- and small-flow conditions are important working conditions that exist objectively during the actual operation. Therefore, based on operational experience, $1.0Q_d$, $1.4Q_d$, and $0.6Q_d$ were selected to analyze cavitation.

The same coordinate scale is selected for different working conditions, so that the difference in every cavitation can be clearly compared and analyzed. As can be seen from Figs. 12, 13, and 14: (1) Under the small-flow $6Q_d$, the vapor volume fraction mainly exists at the blade suction surface and the rear cover and gradually extends to the end of the front cover, rear cover, and the blade suction surface. The cavitation at the inlet of the blade

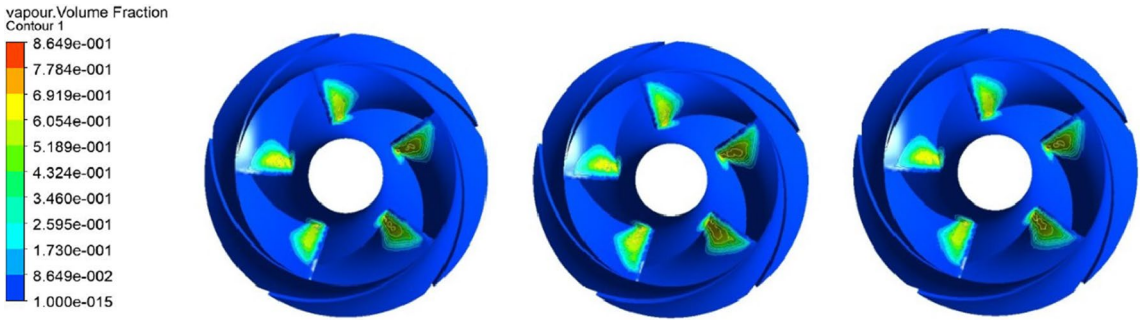

(a) Scheme C2 **(b)** Scheme C3 **(c)** Scheme C4

Fig. 12 Vapor volume distribution of impeller under the $0.6Q_d$ conditions

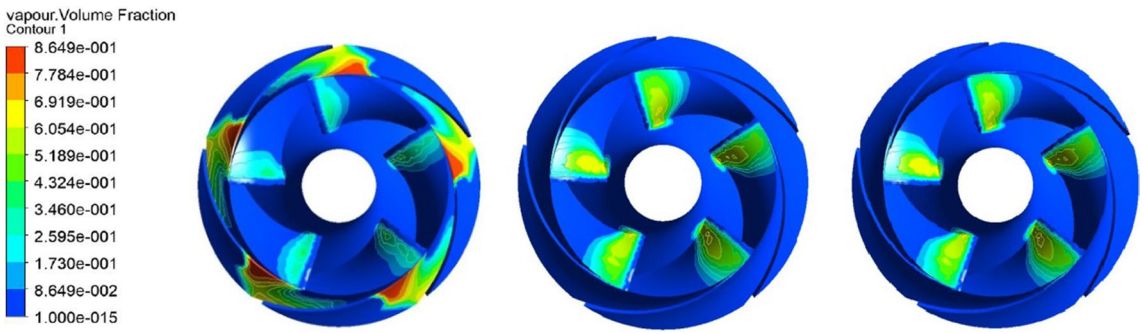

(a) Scheme C2 **(b)** Scheme C3 **(c)** Scheme C4

Fig. 13 Vapor volume distribution of impeller under the design conditions

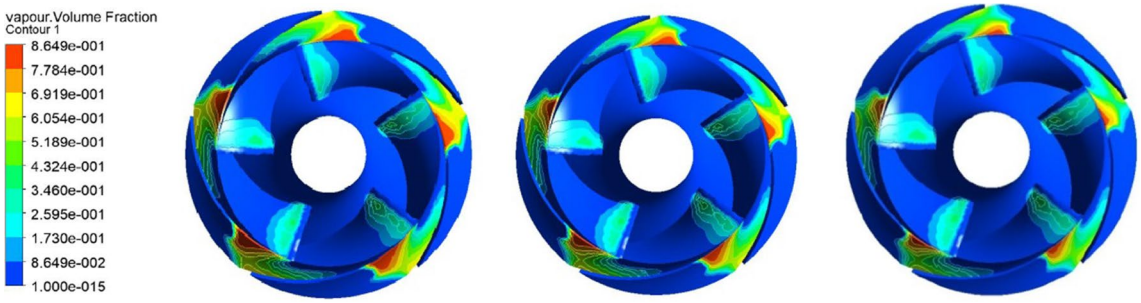

(a) Scheme C2 **(b)** Scheme C3 **(c)** Scheme C4

Fig. 14 Vapor volume distribution of impeller under the $1.4Q_d$ conditions

suction surface is relatively less serious, and the bubbles are mainly concentrated near the rear cover and the inlet of the blade suction surface. It may be due to the high-speed rotation of the impeller, then the centrifugal force spreads it to the outer edge of the impeller, and a low-pressure area near the rear cover is formed. (2) Under the design condition, the vapor volume fraction distribution of scheme C2 has begun to expand and extend, and the overall distribution area is relatively large, mainly located at the end of the blade suction surface and the front of the pressure surface near the front cover. It shows that the different wrap angle matching schemes between the impeller and space diffuser have a great influence on the cavitation state. On the basis of analyzing the hydraulic characteristics, the optimal design for the system of the diagonal-flow pump should be comprehensively evaluated. (3) Under the large-flow $1.4Q_d$, and in the same inlet pressure conditions, the distribution of large-flow $1.4Q_d$ working conditions has been obvious difference, and the overall cavitation situation is serious.

In order to further comprehensively analyze the cavitation under different schemes, a comparative study of scheme B2 and C2 is now conducted, as shown in Fig. 15.

Under the design conditions, the vapor volume distribution area and seriousness of scheme B are larger than scheme C, indicating that the inhibition of impeller cavitation is more obvious as the wrap angle increases within a certain range. When the impeller wrap angle is fixed, the increase in the space diffuser wrap angle also plays a positive role in controlling the impeller cavitation. However, the cavitation volume fraction distribution of scheme C2 has begun to expand and extend. It proves again that the different wrap angle matching schemes between the impeller and space diffuser have great influence on the cavitation. Besides, the optimal design for the system of the diagonal-flow pump should be comprehensively evaluated.

4.4 Pressure Fluctuation Analysis

Pressure fluctuation is closely related to vibration and noise [25]. Its characteristics will cause vibration of the unit, damage the hydraulic components of pump, and affect hydraulic performance and operational stability [26]. The monitoring points are shown in Fig. 16.

Moreover, it is an important indicator to measure the stability of the entire unit. In order to eliminate interference from other factors such as static pressure, introduce a dimensionless pressure coefficient C_p.

$$C_p = \frac{(p - \bar{p})}{\frac{1}{2}\rho u_2^2} \tag{3}$$

where p is the pressure at monitoring point, Pa. $\bar{p}$ is the average pressure at the monitoring point, Pa. ρ is the fluid density, kg/m^3. u is the circumferential velocity at outlet, m/s.

The diagonal-flow pump has five blades with a blade frequency of $5f_n = 242$ Hz. It can be seen from Figs. 17, 18, and 19 that: (1) The peaks in the time domain appear at the integer multiple of blade frequency, and the pressure fluctuation law is not obvious at the monitoring point 1. However, there is a significant difference at the monitoring point 2, and the amplitude decreases gradually from schemes C2 to C4. (2) This phenomenon illustrates that the different space diffuser wrap angles have less influence on fluctuation of the previous fluid, but it has obvious influence on the internal and tail flow of the space diffuser. (3) Within a certain range of

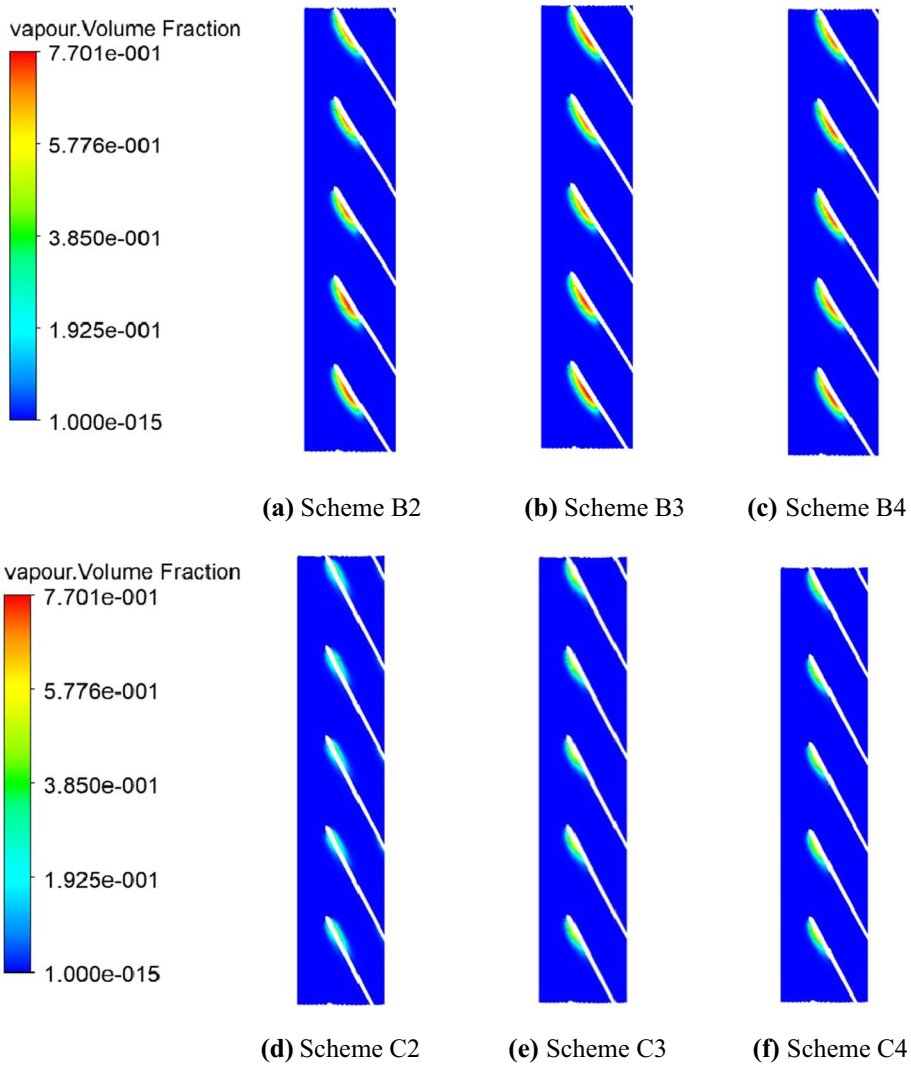

Fig. 15 Vapor volume distribution of impeller surface under the design conditions

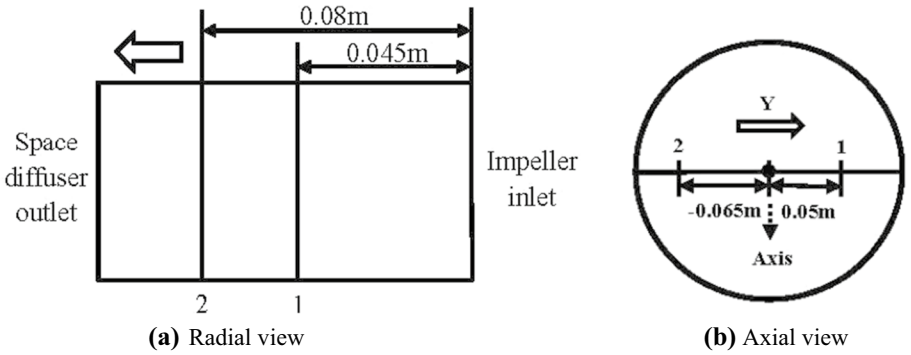

Fig. 16 Monitoring points

wrap angle, the amplitude of pressure fluctuation decreases with the increase in space diffuser wrap angle. The space diffuser can more evenly collect the liquid from the impeller and lead it to the outlet, which improves the flow better with the increase in the space diffuser wrap angle.

The analysis of pressure pulsation will help to combine the hydraulic characteristics analysis and cavitation analysis for optimizing the design of key parameters of pump, and selecting the optimal scheme according to the actual design requirements.

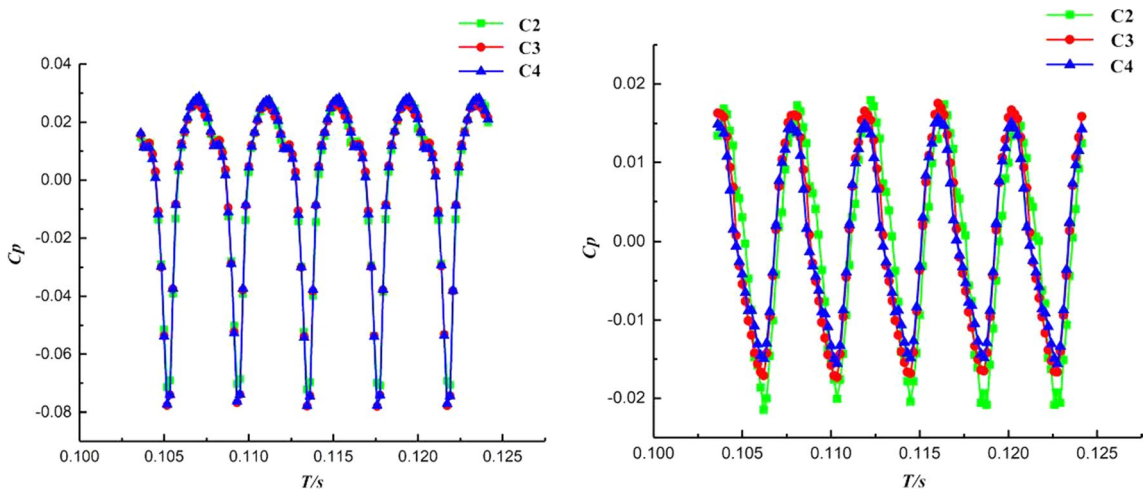

(a) Monitoring point 1 **(b)** Monitoring point 2

Fig. 17 Time domain chart of pressure fluctuation under different schemes

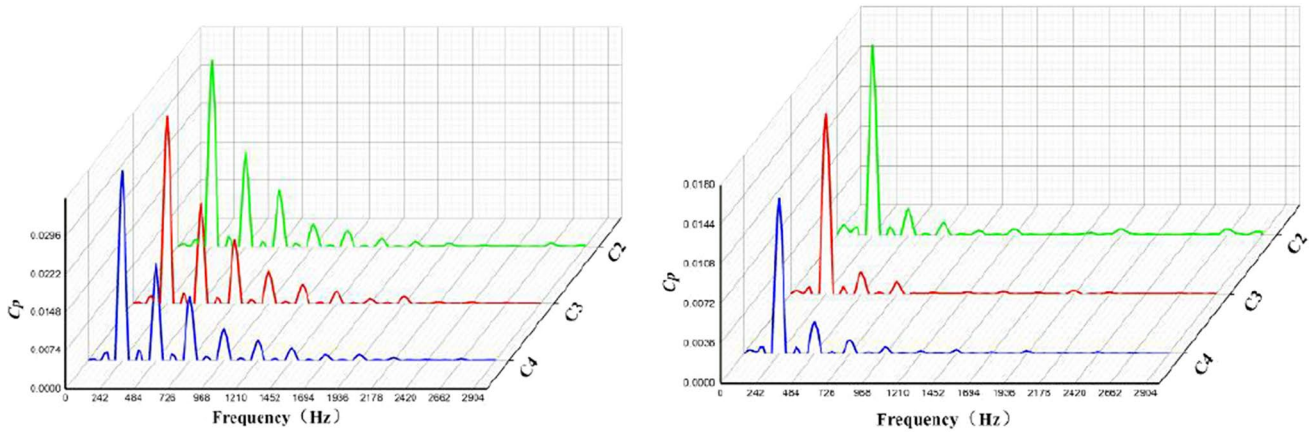

(a) Monitoring point 1 **(b)** Monitoring point 2

Fig. 18 Frequency domain chart of pressure fluctuation under different schemes

5 Conclusion

In the design process of the diagonal-flow pump, the collaborative design between the impeller and space diffuser plays a vital role.

1. The proposed collaborative design process, standardization, and systematic design of R&D process are proved to be effective by each module, which is helpful to reduce the workload greatly and easily find a better balance point about multi-influence of the multi-component parameters. Finally, the optimal matching design between impeller and space diffuser is obtained when the diagonal-flow pump is used in oil and gas field.
2. In a certain angle range, the influence of impeller wrap angle on the diagonal-flow pump is more pronounced than that of the space diffuser angle. So the wrap angle in the collaborative design process should be based on the optimal impeller wrap angle. It is carried out such as the selection of the space diffuser wrap angle by the multidimensional evaluation criteria of collaborative design.
3. Within a certain range of wrap angle, the amplitude of pressure fluctuation decreases with the increase in the space diffuser wrap angle, and the inhibition of impeller cavitation is more obvious as the wrap angle increases. It lays a foundation for the selection of wrap angle and the establishment of the model of law.

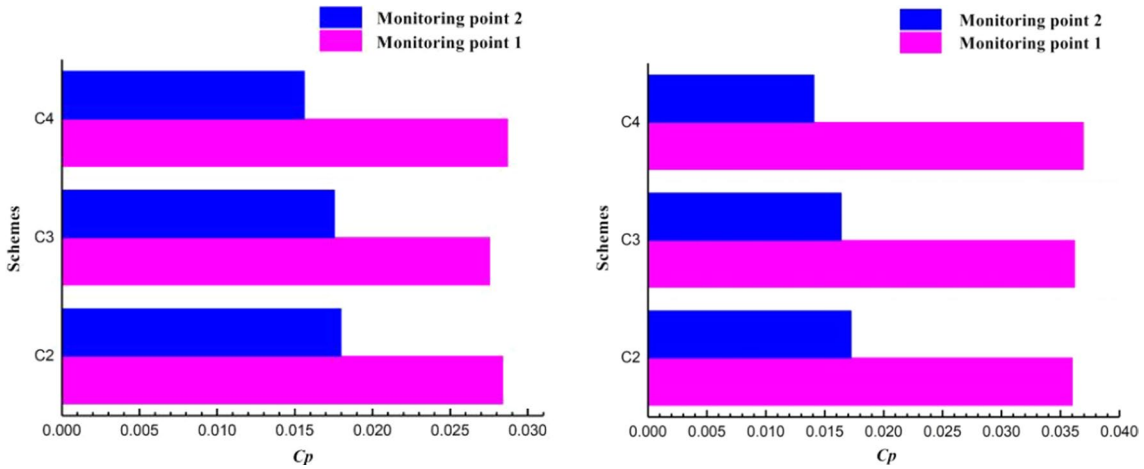

(a) Time domain **(b)** Frequency domain

Fig. 19 Comparison of amplitude points under different schemes

To sum up, collaborative design concept, process model and main idea of the diagonal-pump wrap angles are put forward in this paper. It can quickly and accurately determine the optimal matching scheme and effectively improve the hydraulic performance of the diagonal-flow pump. In future research, the micro-mechanism analysis and macro-characteristic research will be more closely linked, which will improve equipment operating efficiency of oil and gas development.

Acknowledgement The work was supported by the National Key R&D Program of China (No. 2018YFC0310201). The authors also acknowledge the support of National Natural Science Foundation of China (No. 51704254).

References

1. Derakhshan, S.; Pourmahdavi, M.; Abdolahnejad, E.; Reihani, A.; Ojaghi, A.: Numerical shape optimization of a centrifugal pump impeller using artificial bee colony algorithm. Comput. Fluids **81**, 145–151 (2013)
2. Shao, C.; Li, C.; Zhou, J.: Experimental investigation of flow patterns and external performance of a centrifugal pump that transports gas-liquid two-phase mixtures. Int. J. Heat Fluid Flow **71**, 460–469 (2018)
3. Zhu, J.; et al.: Surfactant effect on air/water flow in a multistage electrical submersible pump (ESP). Exp. Therm. Fluid Sci. **98**, 95–111 (2018)
4. Kye, B.; Park, K.; Choi, H.; Lee, M.; Kim, J.H.: Flow characteristics in a volute-type centrifugal pump using large eddy simulation. Int. J. Heat Fluid Flow **72**, 52–60 (2018)
5. Srivastava, S.; Roy, A.K.; Kumar, K.: Design of a mixed flow pump impeller blade and its validation using stress analysis. Procedia Mater. Sci. **6**, 417–424 (2014)
6. Heo, M.W.; Kim, K.Y.; Kim, J.H.; Choi, Y.S.: High-efficiency design of a mixed-flow pump using a surrogate model. J. Mech. Sci. Technol. **30**, 541–547 (2016)
7. Tan, L.; Zhu, B.; Cao, S.; Bing, H.; Wang, Y.: Influence of blade wrap angle on centrifugal pump performance by numerical and experimental study. Chinese J. Mech. Eng. **27**, 171–177 (2014)
8. Liu, M.; Tan, L.; Cao, S.: Influence of geometry of inlet guide vanes on pressure fluctuations of a centrifugal pump. J. Fluids Eng. **140**, 091204 (2018)
9. Kim, J.H.; Ahn, H.J.; Kim, K.Y.: High-efficiency design of a mixed-flow pump. Sci. China Technol. Sci. **53**, 24–27 (2010)
10. Bing, H.; Cao, S.: Experimental study of the influence of flow passage subtle variation on mixed-flow pump performance. Chin. J. Mech. Eng. **27**, 615–621 (2014)
11. Ofuchi, E.M.; et al.: Study of the effect of viscosity on the head and flow rate degradation in different multistage electric submersible pumps using dimensional analysis. J. Pet. Sci. Eng. **156**, 442–450 (2017)
12. Lu, Y.; Wang, X.; Xie, R.: Derivation of the mathematical approach to the radial pump's meridional channel design based on the controlment of the medial axis. Math. Probl. Eng. **2017**, 1–15 (2017)
13. Samad, A.; Kim, K.-Y.; Goel, T.; Haftka, R.T.; Shyy, W.: Multiple surrogate modeling for axial compressor blade shape optimization. J. Propuls. Power **24**, 301–310 (2008)
14. Wang, J.; Wen, S.; Wang, W.; Xi, G.: Intelligence design method for three-dimensional vaned diffusers in a centrifugal compressor. Proc. Inst. Mech. Eng. Part A J. Power Energy **232**, 674–690 (2018)
15. Bonaiuti, D.; Zangeneh, M.: On the coupling of inverse design and optimization techniques for the multiobjective, multipoint design of turbomachinery blades. J. Turbomach. **131**, 021014 (2009)
16. Chen, T.; Sun, Y.B.; Wu, D.Z.; Wang, L.Q.: Cavitation performance improvement of high specific speed mixed-flow pump. IOP Conf. Ser. Earth Environ. Sci. **15**, 0–7 (2012)
17. Kim, J.-H.; Kim, K.-Y.: Analysis and optimization of a vaned diffuser in a mixed flow pump to improve hydrodynamic performance. J. Fluids Eng. **134**, 071104 (2012)
18. Kim, J.H.; Choi, J.H.; Husain, A.; Kim, K.Y.: Multi-objective optimization of a centrifugal compressor impeller through evolutionary algorithms. Proc. Inst. Mech. Eng. Part A J. Power Energy **224**, 711–721 (2010)

19. Ruofu, X.; Zhengwei, W.; Luo, Y.: Stress analysis of Francis turbine runners based on FSI. J. Hydroelectr. Eng. **26**(3), 120–123, 133 (2007)
20. Yakhot, V.; Orszag, S.A.; Thangam, S.; et al.: Development of turbulence models for shear flows by a double expansion technique. J. Phys. Fluids **4**(7), 1510–1520 (1992)
21. Sano, T.; Yoshida, Y.; Tsujimoto, Y.; et al.: Numerical study of rotating stall in a pump vaned diffuser: pump analysis and design. J. ASME J. Fluids Eng. **124**(2), 363–370 (2012)
22. Wang, F.: Research progress of computational model for rotating turbulent flow in fluid machinery. Chin. J Trans. Chin. Soc. Agric. Mach. **47**(02), 1–14 (2016)
23. Bing, H.; Cao, S.; Wang, Y.: Influence of turbulence model on performance prediction of mixed-flow pump. Chin. J. Trans. Chin. Soc. Agric. Mach. **44**(11), 42–47 (2013)
24. Cheng, W.: Research on the Hydraulic Characteristics of Hualong No. 1 Cavity Water Injection-Cooling Pump. D. Xihua University, Chengdu (2018)
25. Liu, Y.; Tan, L.: Tip clearance on pressure fluctuation intensity and vortex characteristic of a mixed flow pump as turbine at pump mode. Renew. Energy **129**, 606–615 (2018)
26. Scheer, H.: Klimawandel und erneuerbare energien. Int. Polit. **59**, 1–6 (2004)